The effects of composite laminate stiffness and loading on stress resultant concentration factor around a hole

Journal:	*Part C: Journal of Mechanical Engineering Science*
Manuscript ID	JMES-17-1220.R1
Manuscript Type:	Original article
Date Submitted by the Author:	11-Dec-2017
Complete List of Authors:	damghani, mahdi; Engineering Design and Mathematics Harrison, Christopher; Atkins Bristol Kennedy, David; Cardiff University
Keywords:	Conformal mapping, Complex variable approach, Stress resultant concentration, Hole, Carbon Fibre Reinforced Polymer
Abstract:	An analytical tool is developed using conformal mapping and the complex variable method for determining the Stress Resultant Concentration Factor (SRCF) in an infinite plate with a circular or elliptical hole. This tool is validated against Finite Element Analysis (FEA). A population space of 305 laminates is generated by stacking uni-directional Carbon Fibre Reinforced Polymer (CFRP) material at various orientations covering a wide spectrum of homogenised stiffness values. The analytical approach is then used to study the effect(s) of loading conditions, stacking sequences and laminate homogenised stiffness values on the SRCF at the edge of a circular hole.

The effects of composite laminate stiffness and loading on stress resultant concentration factor around a hole

M Damghani[*a], **C Harrison**[b], and **D Kennedy**[c]

[a] Engineering Modelling and Simulation Group (EMSG), Engineering Design and Mathematics Department, University of the West of England (UWE), Bristol, UK

[b] Advanced Engineering Unit, Atkins global, Bristol, UK

[c] Engineering Department, Cardiff University, Cardiff, UK

Abstract

An analytical tool is developed using conformal mapping and the complex variable method for determining the Stress Resultant Concentration Factor (SRCF) in an infinite plate with a circular or elliptical hole. This tool is validated against Finite Element Analysis (FEA). A population space of 305 laminates is generated by stacking uni-directional Carbon Fibre Reinforced Polymer (CFRP) material at various orientations covering a wide spectrum of homogenised stiffness values. The analytical approach is then used to study the effect(s) of loading conditions, stacking sequences and laminate homogenised stiffness values on the SRCF at the edge of a circular hole.

Keywords: Conformal mapping, Complex variable approach, Stress resultant concentration, Carbon Fibre Reinforced Polymer, Hole

[*] *Corresponding author: Engineering Modelling and Simulation Group (EMSG), Engineering Design and Mathematics Department, University of the West of England (UWE), Bristol, UK*

Email:Mahdi.Damghani@uwe.ac.uk

1 Introduction

Composite materials are widely used in the aerospace industry for high performance components. For instance, more than 50% of Airbus A350 and Boeing 787 passenger aircraft are made of such materials. Composites are also finding applications as load bearing structural components in other industries amongst which are defence, automotive, marine, oil and gas, rail and civil engineering. Due to the high stiffness to weight ratio of such materials compared to conventional metallic materials such as aluminium, the use of composites can lead to significant weight saving which in turn brings about improved performance and reduction in fuel consumption. In order to use the full potential of such materials, it is essential to better understand and characterise their behaviour.

As the result of design requirements and practicality of use, the existence of holes is inevitable in composite structures such as windows in the aircraft fuselage, access-holes in the wing, drilled holes for bolted and riveted connections etc. It is well known that elevated stresses give rise to stress/strain concentrations occurring at the vicinity of holes making them prone to crack initiation and propagation. The quantity of such stresses is dependent on the geometry of a hole, loading conditions, stiffness and anisotropy of the composite laminate.

There have been numerous attempts in obtaining Stress Concentration Factor (SCF) at the boundary of a hole/notch in laminated composite plates. Some of such works make use of numerical approaches such as Finite Element Analysis (FEA) [1–5] whilst others focus on the use of fast and precise analytical methods [6–15]. Experimental techniques compliment the two previous approaches and have been used extensively to validate both analytical and numerical solutions.

The majority of the analytical works in the literature focus on the methods of determination of stress state around a hole and are based on the work of Muskhelishvili [15] and Savin [16]. For example, Bonora et al. [6,7] provided closed form solutions for stress

state around circular and elliptical holes in laminated composite plates using the classic Airy solution method. Amongst similar works are the works of Chauhan et al. [10]. They employed an analytical complex variable method and studied the effect of stacking sequence on tangential stresses around a rectangular hole under uni-axial loading for a finite Graphite/Epoxy composite plate. For their laminate of study, they concluded that maximum and minimum SCF take place for $[0_8]_s$ and $[90_8]_s$ lay-up, respectively. Sharma [17] studied the effect of fibre orientation, for both Graphite/Epoxy and Carbon/Epoxy composite laminates, under uni-axial loading on stress pattern at the edge of a polygonal hole. He concluded that minimum and maximum SCF around the hole occurs for 90^o and 0^o fibre angles, respectively. Russo et al. [13] performed a parametric study of SCF in both Glass Fibre Reinforced Polymer (GFRP) and Carbon Fibre Reinforced Polymer (CFRP) containing a circular hole both analytically and experimentally. Hufenbach et al. [14] used a complex variable method and mapping functions to obtain stress fields around circular and elliptical holes in a finite Glass-Fibre-Polypropylene (GF/PP) composite plate. Excellent agreement was established between the proposed analytical method and experimental results. Although SCF around circular/elliptical holes represents the case in most engineering applications, but some researchers investigated SCF around holes of various other shapes such as triangular [18,19], rectangular [11], hypocycloidal [10], polygonal[17,20] and irregular[21,22] holes.

The use of closed form analytical solutions to determine SCF in geometrically complex structures and general loading scenarios is very difficult and hence the FEA is often adopted. For instance, Jain et al. [23] employed FEA and studied the effect of hole diameter to plate width of rectangular isotropic, orthotropic and laminated composite plates with central circular hole under different transverse static loading conditions. Khechai et al. [24] evaluated the stress distribution around circular holes in thin isotropic and symmetric laminated plates, subjected to uniaxial loading by using a specially formulated quadrilateral finite element. Othman et al. [25] used FEA and the concept of

Defence Hole System (DHS) to reduce stress concentration in holes of composite bolted joints. Darwish et al. [26,27] used three dimensional FEA to formulate stress concentration around circular countersunk holes in composite orthotropic plates under uniaxial loading.

Experimental techniques have been used to obtain SCF in plates having circular holes. Makki et al. [1] performed uniaxial testing of both steel plates and orthotropic CFRP laminates and measured stress concentration factor for circular holes of various dimensions using Digital Image Correlation (DIC) technique. The result given by the DIC camera was identical with the FEA results for isotropic materials. On the contrary, for orthotropic materials, the results of the DIC method were not coherent with the FEA and the literature values, which reflected on the anisotropic character of the composite material. DIC technique was used by Zhao et al. [28] to evaluate stress field around circular hole in thermoplastic orthotropic composite plates. They observed good correlation of numerical results with those of experimental procedure.

Despite considerable amount of attention in developing analytical, numerical and experimental methods, a comprehensive parametric study on a large number of laminated composite structures demonstrating the effects of stiffness of structure and the loading condition on the Stress Resultant Concentration Factor (SRCF) has received little attention with scarce amount of scientific data in the subject area. To achieve such an objective, the use of fast and computationally efficient methods has clear advantage over labour intensive and computationally expensive numerical and FEA.

Therefore, in the present paper, the authors address such shortcomings and lack of data via the use of analytical approach. The approach employs the well-established complex variable method for anisotropic material and is utilised to obtain stress resultant distribution and Stress Resultant Concentration Factor (SRCF) at the edge of an elliptical or circular hole in an infinite composite plate under membrane loading,

which is the dominant loading and boundary condition for thin structures (see Section 2 for a brief review of the theory and the expressions for the stress components for any combination of membrane loading). The analytical formulation is embedded in Excel software [29] with a Visual Basic macro and validated by FEA using MSC Nastran 2014 [30] (see Section 3 for details of validation). The approved analytical solution is used for a parametric study of the influence of composite laminate stiffness on SRCF around a circular hole for several loading conditions on 305 composite laminates. The results of the parametric study are presented in Section 4.

2 Methodology

In this study, conformal mapping, i.e. mapping that preserves angles, and the complex variable approach is used to determine stresses at the edge of a circular or elliptical hole in an infinite composite plate subject to remote membrane forces. It is assumed that the plate is in a plane stress state and body forces are absent. It is further assumed that the plate material remains in its linear elastic state. The effects of out of plane loading are not considered in the current study.

The stress-strain relationship in a composite material is defined as [6,7,17,31]:

$$\begin{Bmatrix} N \\ M \end{Bmatrix} = \begin{bmatrix} A & B \\ B & D \end{bmatrix} \begin{Bmatrix} \varepsilon^0 \\ \kappa \end{Bmatrix} \quad (1)$$

where $[A]$, $[B]$ and $[D]$ are extensional, extensional-bending coupling and bending stiffness matrices, respectively. $\{\varepsilon^0\}$ and $\{\kappa\}$ are strain and curvature matrices at the mid-plane of the composite laminate, respectively. $\{N\}$ and $\{M\}$ are 3x1 matrices of membrane and out of plane bending loading, also known as stress resultants, with units of force per unit width and moment per unit width, respectively. Stress resultants are defined as:

$$N_x = \int_{-\frac{h}{2}}^{\frac{h}{2}} \sigma_x dz,\ N_y = \int_{-\frac{h}{2}}^{\frac{h}{2}} \sigma_y dz,\ N_{xy} = \int_{-\frac{h}{2}}^{\frac{h}{2}} \tau_{xy} dx \tag{2}$$

where σ_x, σ_y and τ_{xy} are direct normal and shear stresses through the laminate thickness. In order to obtain the compliance matrix of a composite material, the ABD matrix in the above equation is inverted, yielding:

$$\begin{Bmatrix} \varepsilon^0 \\ \kappa \end{Bmatrix} = \begin{bmatrix} a & b \\ b & d \end{bmatrix} \begin{Bmatrix} N \\ M \end{Bmatrix} \tag{3}$$

where the abd matrix is the compliance matrix with the following elements:

$$\begin{aligned} [a] &= [A]^{-1} + [A]^{-1}[B]\left([D] - [B][A]^{-1}[B]\right)^{-1}[B][A]^{-1} \\ [b] &= -[A]^{-1}[B]\left([D] - [B][A]^{-1}[B]\right)^{-1} \\ [d] &= \left([D] - [B][A]^{-1}[B]\right)^{-1} \end{aligned} \tag{4}$$

For simplicity, the composite laminate is assumed to be symmetric. Therefore, the membrane-bending coupling terms vanish, i.e. $[b] = 0$, and composite laminate mid-plane strains can be expressed as:

$$\begin{aligned} \varepsilon_x &= a_{11}N_x + a_{12}N_y + a_{16}N_{xy} \\ \varepsilon_y &= a_{12}N_x + a_{22}N_y + a_{26}N_{xy} \\ \gamma_{xy} &= a_{16}N_x + a_{26}N_y + a_{66}N_{xy} \end{aligned} \tag{5}$$

where $a_{ij}\,(i, j = 1,2,6)$ coefficients are elements in the compliance matrix.

In the absence of body forces, stress resultants can be defined using Airy's stress function $U(x, y)$ as follows:

$$N_x = t\frac{\partial^2 U}{\partial y^2},\ N_y = t\frac{\partial^2 U}{\partial x^2},\ N_{xy} = -t\frac{\partial^2 U}{\partial x \partial y} \tag{6}$$

where t is the thickness of the composite laminate. It is worth noting that in the proposed analytical solution, the authors use the concept of stress resultants of Eq. (2)

instead of composite ply level stresses. This is due to the use of Airy stress functions that are suitable for two dimensional plane stress/plane strain problems, where stress is assumed to be constant through the thickness. However, for composite laminate structures, the stress through the thickness is not constant and has discontinuous distribution. The use of stress resultant overcomes such limitation. Stress resultants are crucial for quantifying static and fatigue strength of composite structures. For instance, in static analysis they can be used to predict the notched strength of composite laminates containing circular holes and straight cracks based on either the ‘‘point stress’’ criterion or the ‘‘average stress’’ criterion. The reader is referred to Pandita et al. [32] for further details.

We also know that (from the compatibility of strains in a two dimensional space):

$$\frac{\partial^2 \varepsilon_x}{\partial y^2} + \frac{\partial^2 \varepsilon_y}{\partial x^2} = \frac{\partial^2 \gamma_{xy}}{\partial x \partial y} \tag{7}$$

Combining the above equations leads to:

$$a_{22}\frac{\partial^4 U}{\partial x^4} - 2a_{26}\frac{\partial^4 U}{\partial x^3 \partial y} + (2a_{12} + a_{66})\frac{\partial^4 U}{\partial x^2 \partial y^2} - 2a_{16}\frac{\partial^4 U}{\partial x \partial y^3} + a_{11}\frac{\partial^4 U}{\partial y^4} = 0 \tag{8}$$

Lekhnitskii [33] demonstrated that to solve two-dimensional anisotropic problems, it is essential to solve the following characteristic equation:

$$a_{11}S^4 - 2a_{16}S^3 + (2a_{12} + a_{66})S^2 - 2a_{26}S + a_{22} = 0 \tag{9}$$

The roots of the characteristic equation, also known as complex values of anisotropy, have complex values and are in conjugate pairs as:

$$\begin{aligned} s_1 &= \alpha_1 + i\beta_1; s_3 = \overline{s_1} \\ s_2 &= \alpha_2 + i\beta_2; s_4 = \overline{s_2} \end{aligned} \tag{10}$$

Airy’s stress function can be represented by arbitrary functions of X_k of variables z_k as follows:

$$U(x,y) = X_1(z_1) + X_2(z_2) + \overline{X_1(z_1)} + \overline{X_2(z_2)}$$
$$z_1 = x + s_1 y = x + \alpha_1 y + i\beta_1 y \quad (11)$$
$$z_2 = x + s_2 y = x + \alpha_2 y + i\beta_2 y$$

and defining $\phi(z_1)$ and $\psi(z_2)$ as:

$$\frac{dX_1}{dz_1} = \phi(z_1),\ \frac{dX_2}{dz_2} = \psi(z_2),\ \frac{d\overline{X_1}}{dz_1} = \overline{\phi(z_1)},\ \frac{d\overline{X_2}}{dz_2} = \overline{\psi(z_2)} \quad (12)$$

$\phi(z_1)$ and $\psi(z_2)$ are analytic functions which suggests that they have continuous partial derivatives within their domain. Stress resultant components in terms of $\phi(z_1)$ and $\psi(z_2)$, can be calculated as:

$$N_x = 2\,\mathrm{Re}\left[s_1^2\phi_0'(z_1) + s_2^2\psi_0'(z_2)\right]$$
$$N_y = 2\,\mathrm{Re}\left[\phi_0'(z_1) + \psi_0'(z_2)\right] \quad (13)$$
$$N_{xy} = -2\,\mathrm{Re}\left[s_1\phi_0'(z_1) + s_2\psi_0'(z_2)\right]$$

For the sake of conciseness, the reader is referred to Appendix A for details of obtaining mapping, analytic and stress functions.

2.1 Material and lay-up

In order to study the effects of SRCF on various composite laminates with a range of stiffness values, a uni-directional composite ply with mechanical properties given in Table 1 is used.

Three hundred and five balanced and symmetric stacking sequences are generated, by assuming a laminate with 28 plies, to cover a wide spectrum of composite laminates with various homogenised stiffness values, i.e. shear modulus and modulus in x and y directions. The population of stacking sequences had a homogenised shear modulus ranging from 5.58GPa to 27.51GPa and direct modulus ranging from 10GPa to 120GPa.

3 Validation of the analytical method with FEA

MSC Nastran was used to perform FEA. The plate is modelled using the boundary conditions and loading represented in Fig. 1. F_x and F_y point forces are distributed to the plate structure using RBE3 elements. RBE3 elements are interpolation constraint elements that define the motion at a reference grid point, i.e. hole centre, as the weighted average of the motions at a set of other grid points, i.e. hole edge. The structure is constrained (grounded) at the middle of the hole. Since the master node of RBE3 elements at the location of the hole cannot be grounded, this node is connected to a very rigid spring element (CBUSH element) of zero length. The other end of CBUSH element is then constrained in all degrees of freedom.

The validation is performed for material, composite lay-up, hole geometry, and loading type given in Table 2. Hereafter, Parameter λ is defined as the ratio of loading in y direction to that of x direction ($\lambda = N_y / N_x$). In all validation runs, values of applied loads are $N_x = 280N/mm$ ($\lambda = 0$), $N_x = N_y = 280N/mm$ ($\lambda = 1$), for uni-axial and bi-axial loading conditions, respectively.

The contour plot of output stresses, i.e. average normal stresses in x and y direction and average shear stress in xy plane, at the edge of circular hole for bi-axial loading (see Val-A in Table 2) and uni-axial loading (see Val-B in Table 2) is given in Fig. 2 and Fig. 3, respectively. Comparison of analytical method with the numerical approach is given in Fig. 4 and Fig. 5. These figures illustrate excellent agreement of FE results with those of analytical approach.

4 Results and discussions

The objective of this study is to investigate the effect(s) of composite laminate stiffness, resulting from different stacking sequences, and loading conditions on the quantity of SRCF at the edge of a hole. The SRCF is important in the design of composite

structures when quantifying static or fatigue strength. A circular hole with radius of 10mm is considered hereafter, representative of a bolt or rivet hole in a typical aerospace structure.

Fig. 6 shows SRCF for various quantities of E_x / E_y (homogenised stiffness values of composite laminate in x and y directions) under uni-axial loading. The SRCF in this context is defined as the ratio of maximum tangential stress resultant (N/mm) at the edge of the hole to the remote applied stress resultant, i.e. $SRCF = N_\theta \Big/ \sqrt{N_x^2 + N_y^2}$. It should be noted, for interpretation of the results, SRCF values represent average stress concentration times the thickness of homogenised section rather than ply level stresses.

It is evident from the graph that for all homogenised shear modulus values of the laminate, the SRCF decreases with the decrease in the ratio of E_x / E_y . In other words, reducing the stiffness in the direction of applied load brings about less stress resultant concentration around the edge of the hole. The graph also suggests, for uni-axial loading, introduction of angle plies in the stacking sequence leads to an increase in homogenised shear modulus bringing about the reduction of SRCF. One noticeable observation is the increase of SRCF for some shear moduli in the interval E_x / E_y <0.3. This is mainly due to the use of stacking sequences with a dominant number of plies in 90^o angle and no plies at 0^o angle (0^o plies have fibres parallel to loading direction). For example, increase of SRCF from 2.99 to 3.46 is associated with E_x / E_y =0.16 and E_x / E_y =0.08 for G_{xy} =5.58GPa pertinent to stacking sequences of $(90_{13}/0)_s$ and $(90)_{28}$, respectively. This phenomenon is associated with a shift in the position of the point with the highest SRCF around the edge of hole as demonstrated in Fig. 7. For all stacking sequences, maximum SRCF takes place at 90^o angle from the load direction; however, for laminates with a dominant number of 90^o and no 0^o plies, this angle becomes zero.

Such extremes of anisotropy are not common in engineering structures as they reduce performance in other aspects such as tolerance to impact.

The use of more angle plies increases the homogenised shear modulus of a composite laminate leading to less stiff laminates in the loading direction, i.e. smaller value of E_x. In this study, the laminates having high homogenised shear modulus are generated by using solely angle plies with mechanical properties given in Table 3, i.e. $((15/-15)_7)_s$, $((30/-30)_7)_s$, $((45/-45)_7)_s$, $((60/-60)_7)_s$, $((75/-75)_7)_s$. Such laminates do not possess any 0^o and 90^o plies and they represent only one point in the graphs of Fig. 6. Therefore, they are studied separately as shown in Fig. 8. This figure shows that minimum SRCF of 2.61 takes place for the situation where all plies have 60^o orientation, i.e. $((60/-60)_7)_s$ for uni-axial loading. It is worth noting that this stacking sequence does not have the highest homogenised shear modulus. Thus, this observation suggests that, in the absence of 0^o and 90^o plies, the highest homogenised shear modulus, i.e. $((45/-45)_7)_s$, does not necessarily give the lowest SRCF. Moreover, it is evident from the graph that as the plies angle increases from 15^o to 75^o, the angle made between the direction of loading and the point with highest SRCF decreases from 90^0 to 0^o, respectively. However, introduction of 0^o or 90^o plies enforces the laminate to have SRCF either at 0^o or 90^o depending on the number of plies used in those directions. Fig. 9 and Fig. 10 illustrate the quantity of SRCF for various values of E_x / E_y for bi-axial loading of λ =0.5 and λ =-0.5, respectively. In all figures, N_x is assumed to be always in tension (positive) and N_y is either in compression (negative) or in tension depending on the sign of λ. The general trend, in both cases, suggests that increase in homogenised shear modulus of laminate (G_{xy}) leads to lower SRCF. However, for a given G_{xy} and λ =0.5 (Fig. 9), the lower the ratio of E_x / E_y the lower the SRCF becomes. When λ

=-0.5 (Fig. 10), the combined effect of tension and compression loading results in minimal SRCF at around E_x / E_y =0.5 for most laminates.

As illustrated in Fig. 11 and Fig. 12, in purely angle ply laminates, minimum SRCF of 1.90 and 2.71 occur for stacking sequences $((75/-75)_7)_s$ and $((45/-45)_7)_s$ at λ =0.5 and λ =-0.5, respectively. As mentioned previously, G_{xy} for stacking sequence $((75/-75)_7)_s$ is 12.00 GPa as opposed to 31.23 GPa associated to $((45/-45)_7)_s$. However, in this particular case, the minimum SRCF does not occur for the laminate with the highest G_{xy}. This could be due to the Poisson's ratio effect. For instance, for $((75/-75)_7)_s$ with λ =0.5, N_x produces tensile and compressive strains in x and y directions, respectively. On the contrary, N_y produces tensile strain in y and compressive strain in x direction. Superimposing these strains and considering Poisson's ratio of the laminate as υ_{yx}=0.09 and υ_{xy}=0.85 suggests relief in load intensity in x direction leading to a lower SRCF compared to that of $((45/-45)_7)_s$ and λ =-0.5. On the other hand, when stacking sequence is $((45/-45)_7)_s$ and λ =-0.5, considering υ_{yx}=0.72 and υ_{xy}=0.72, tensile load in the x direction brings about tensile strain in the x and compressive strain in the y direction whereas compressive load in y direction causes the laminate to undergo compressive strain in the y direction and tensile strain in the x direction. This, along with equal Poisson's ratio in both directions leads to intensification of load in the x direction bringing about SRCF of 2.71. It is worth noting that the loading condition, i.e. bi-axial, has shifted the location of point with highest SRCF around the edge of the hole.

Fig. 13 and Fig. 14 illustrate the quantity of SRCF for various values of E_x / E_y for bi-axial loading of λ =-1.00 and λ =1.00, respectively. As depicted in Fig. 13, for λ =-

1.00, an apparent decrease of SRCF with increase of G_{xy} is noticeable. For this case E_x / E_y =1 gives the lowest SRCF for all laminates and beyond this point SRCF increases. However, strange behaviour is observed for λ =1.00 as shown in Fig. 14. For this case, increase of G_{xy} up to 16.55GPa is accompanied by reduction of SRCF. Despite increase of G_{xy} from 19.29GPa to 27.51GPa, SRCF increases.

Fig. 15, Fig. 16 and Fig. 17 illustrate combined effects of loading ratio λ and laminate stiffness ratio, i.e. E_x / E_y, on SRCF for three homogenised shear modulus values of G_{xy} =5.58GPa, G_{xy} =16.58GPa and G_{xy} =23.86GPa, that represent low, medium and high shear stiffness values within the laminates population space of study, respectively. Fig. 15a and Fig. 15b both show that the positive λ generally yields lower SRCF with the minimum being 1.96 pertinent to λ =1.5. It is evident from the graph that for λ <0, SRCF becomes minimum at an E_x / E_y ratio close to value of $|\lambda|$. For example, minimum SRCF for λ =-2.0, λ =-1.5 and λ =-0.5 takes place at E_x / E_y =2.11, 1.63 and 0.47, respectively. A similar trend can be observed in Fig. 16 and Fig. 17 as G_{xy} increases from 5.58GPa to 16.58GPa and 23.86GPa. In most cases, the lowest SRCF for all shear moduli occurs when λ =1.0.

5 Conclusions

The analytical tool was used to visualise the effect of laminate anisotropy and loading direction on the SRCF around a circular hole in an infinite plate. This was achieved by creating a population of laminates and loadings that are representative of thin-walled panels used in the aerospace industry. It is expected that similar graphs can be used by designers of composite structures to optimise the laminate geometry in the regions of holes. This further enables efficient laminates without resorting to complicated mathematics or time-consuming FEA.

It was shown that composite laminates demonstrate a very complex behaviour towards loading, stacking sequence, i.e. resulting in homogenised stiffness, and SRCF. In the absence of purely angle ply laminates, it was demonstrated that increase in homogenised shear modulus of laminate leads to reduction in SRCF. However, this cannot hold true for angle ply laminates as the effects of Poisson ratio becomes predominant. Finally, it was illustrated that positive λ yield the lowest SRCF compared to other types of loading investigated in this study.

Appendix A

A1 Mapping function

The conformal mapping function is used to map the infinite area external to the hole in a complex Z-plane, i.e. $z=x+iy$, onto the external area of a unit circle ($|\zeta|>1$) in the ζ -plane, i.e. $\zeta=\xi+i\eta$, or in the polar format as $\zeta=\rho e^{i\theta}$, as illustrated in Fig. A1. The mapping function that conformably maps an elliptical hole having major axis a and minor axis b onto a unit circle for an isotropic material is as follows:

$$z=\omega(\zeta)=R\left(\zeta+\frac{m}{\zeta}\right)$$
$$m=\frac{a-b}{a+b};R=\frac{a+b}{2} \quad \text{(A1)}$$

For anisotropic materials due to a fully populated compliance matrix, deformations go through affine transformation. Therefore, by incorporating complex values of anisotropy, i.e. replacing i with s_1 and s_2, the mapping function becomes:

$$z=\omega(\zeta)=R\left(\zeta+\frac{m}{\zeta}\right)=R\left[\left(m+\rho^2\right)\cos\theta+s_j\left(\rho^2-m\right)\sin\theta\right] \quad \text{(A2)}$$

After simplification and considering that $\cos\theta=\frac{1}{2}\left(\frac{\zeta}{\rho}+\frac{\rho}{\zeta}\right)$ and $\sin\theta=\frac{-i}{2}\left(\frac{\zeta}{\rho}-\frac{\rho}{\zeta}\right)$ the above equation for anisotropic materials takes the form:

$$z_j = \omega_j(\zeta) = \frac{R}{2}\left[n_j\left(\frac{\rho^2}{\zeta} + \frac{m\zeta}{\rho^2}\right) + n_j^*\left(\frac{m}{\zeta} + \zeta\right)\right]$$
$$n_j = 1 + is_j; j = 1,2 \quad \text{(A3)}$$
$$n_j^* = 1 - is_j$$

For the edge of the hole, i.e. $|\zeta| = 1$, Eq. (A3) simplifies to:

$$z_j = \omega_j(\zeta) = \frac{R}{2}\left[n_j\left(\frac{1}{\zeta} + m\zeta\right) + n_j^*\left(\frac{m}{\zeta} + \zeta\right)\right] \quad \text{(A4)}$$

A2 Calculation of stress functions

The existence of a discontinuity such as a hole in the plate alters the stress field in the plate. In order to obtain the stress function for such a problem and due to linear and elastic behaviour of the material, the principle of superposition is used. The problem is split into two stages as follows:

A2.1 Stage 1

At this stage, the plate without a hole subjected to remote external loading N_x^R, N_y^R and N_{xy}^R is considered. The fictitious boundary conditions at the location of the hole are regarded as g_1 and g_2 as shown in Fig. A2.

Stress functions to be determined for this stage are $\phi_1(z_1)$ and $\psi_1(z_2)$ satisfying g_1 and g_2 boundary conditions. In order to obtain stress functions for this stage the following is assumed:

$$\phi_1'(z_1) = E$$
$$\psi_1'(z_2) = F + Gi \quad \text{(A5)}$$

Therefore, we have:

$$\phi_1(z_1) = Ez_1$$
$$\psi_1(z_2) = (F + Gi)z_2 \quad \text{(A6)}$$

where E, F and G are real value constants that will be determined by substituting Eq. (A5) into Eq. (13):

$$E = \frac{N_x + (\alpha_2^2 + \beta_2^2)N_y + 2\alpha_2 N_{xy}}{2\left[(\alpha_2 - \alpha_1)^2 - (\beta_1^2 - \beta_2^2)\right]}$$
$$F = \frac{(\alpha_1^2 - \beta_1^2 - 2\alpha_1\alpha_2)N_y - N_x - 2\alpha_2 N_{xy}}{2\left[(\alpha_2 - \alpha_1)^2 - (\beta_1^2 - \beta_2^2)\right]} \quad \text{(A7)}$$
$$G = \frac{0.5N_{xy} + F\alpha_2 + E\alpha_1}{\beta_2}$$

The resultant of forces, i.e. boundary conditions, around the contour of fictitious hole in ζ -plane is represented as:

$$g_1 = 2\,\mathrm{Re}\left[\phi_1(z_1) + \psi_1(z_2)\right]$$
$$g_2 = 2\,\mathrm{Re}\left[s_1\phi_1(z_1) + s_2\psi_1(z_2)\right] \quad \text{(A8)}$$

Therefore:

$$g_1 = 2\,\mathrm{Re}\left[Ez_1 + (F + Gi)z_2\right]$$
$$g_2 = 2\,\mathrm{Re}\left[s_1 Ez_1 + s_2(F + Gi)z_2\right] \quad \text{(A9)}$$

A2.2 Stage 2

This stage considers the plate with the hole in the absence of remote loading. Stress functions to be determined for this stage are $\phi_2(z_1)$ and $\psi_2(z_2)$ satisfying some boundary conditions. In order to obtain the solution for which the total loads on the contour of the hole are zero, i.e. traction free boundary condition on which only tangential stresses exist and therefore shear and radial stresses vanish, it is essential for the boundary condition at the edge of the hole to be $g_1' = -g_1$ and $g_2' = -g_2$. In other words, boundary conditions are equal and opposite signs of stage 1, as shown in Fig. A2. Hence;

$$g_1' = -2\,\mathrm{Re}\left[Ez_1 + (F + Gi)z_2\right]$$
$$g_2' = -2\,\mathrm{Re}\left[s_1 Ez_1 + s_2(F + Gi)z_2\right] \quad \text{(A10)}$$

By expanding the term and considering that $\overline{r+\frac{m}{r}}=\frac{1}{r}+mr$ for $r=\zeta=e^{i\theta}$ we have:

$$g_1^{'}=-\left[\left(H_1+\overline{H_2}\right)\left(\frac{1}{r}+mr\right)+\left(H_2+\overline{H_1}\right)\left(r+\frac{m}{r}\right)\right]$$
$$g_2^{'}=-\left[\left(H_3+\overline{H_4}\right)\left(\frac{1}{r}+mr\right)+\left(H_4+\overline{H_3}\right)\left(r+\frac{m}{r}\right)\right] \quad \text{(A11)}$$

where

$$H_1=\frac{R}{2}\left[En_1+\left(F+iG\right)n_2\right]$$
$$H_2=\frac{R}{2}\left[En*_1+\left(F+iG\right)n*_2\right]$$
$$H_3=\frac{R}{2}\left[s_1En_1+s_2\left(F+iG\right)n_2\right] \quad \text{(A12)}$$
$$H_4=\frac{R}{2}\left[s_1En*_1+s_2\left(F+iG\right)n*_2\right]$$

Based on Sharma et al. [17], the Schwarz Integral Formula is used for calculation of stress functions in the absence of remote loading in conjunction with boundary conditions $g_1^{'}$ and $g_2^{'}$ as below:

$$\phi_2(\xi)=\frac{i}{4\pi\left(s_1-s_2\right)}\oint_{|\xi|=1}\left(s_2g_1^{'}-g_2^{'}\right)\frac{r+\zeta}{r-\zeta}\frac{dr}{r}+\lambda_1$$
$$\psi_2(\xi)=\frac{-i}{4\pi\left(s_1-s_2\right)}\oint_{|\xi|=1}\left(s_1g_1^{'}-g_2^{'}\right)\frac{r+\zeta}{r-\zeta}\frac{dr}{r}+\lambda_2 \quad \text{(A13)}$$

where λ_1 and λ_2 are some imaginary constants that have no impact on stress field so can be ignored. ζ is an arbitrary point of the plane of a complex variable. $r=e^{i\theta}$ is the boundary value of ζ on the circle of unit radius. Considering;

$$\oint_{|\zeta|=1}\frac{1}{r^k}.\frac{r+\zeta}{r-\zeta}.\frac{dr}{r}=\frac{4\pi i}{\zeta^k},\ \oint_{|\zeta|=1}r^k.\frac{r+\zeta}{r-\zeta}.\frac{dr}{r}=0 \quad \text{(A14)}$$

Therefore, the stress function for the second stage in terms of ζ becomes:

$$\phi_2(\zeta)=\left[\frac{l_1}{\zeta}+\frac{l_2 m}{\zeta}\right]$$
$$\psi_2(\zeta)=-\left[\frac{l_3}{\zeta}+\frac{l_4 m}{\zeta}\right] \quad \text{(A15)}$$

where;

$$l_1=\frac{1}{s_1-s_2}\left[s_2\left(H_1+\overline{H_2}\right)-\left(H_3+\overline{H_4}\right)\right]$$
$$l_2=\frac{1}{s_1-s_2}\left[s_2\left(H_2+\overline{H_1}\right)-\left(H_4+\overline{H_3}\right)\right]$$
$$l_3=\frac{1}{s_1-s_2}\left[s_1\left(H_1+\overline{H_2}\right)-\left(H_3+\overline{H_4}\right)\right] \quad \text{(A16)}$$
$$l_4=\frac{1}{s_1-s_2}\left[s_1\left(H_2+\overline{H_1}\right)-\left(H_4+\overline{H_3}\right)\right]$$

A3 Final stress function

The final stress function of the problem is the summation of previously obtained stress functions as:

$$\phi(z_1)=\phi_1(z_1)+\phi_2(z_1)$$
$$\psi(z_2)=\psi_1(z_2)+\psi_2(z_2) \quad \text{(A17)}$$

By combining Eqs (12), (A5), (A14) and (A16), the final resultant force components are calculated as;

$$N_x=N_x^R+2\,\mathrm{Re}\left[s_1^2\phi_2'(z_1)+s_2^2\psi_2'(z_2)\right]$$
$$N_y=N_y^R+2\,\mathrm{Re}\left[\phi_2'(z_1)+\psi_2'(z_2)\right] \quad \text{(A18)}$$
$$N_{xy}=N_{xy}^R-2\,\mathrm{Re}\left[s_1\phi_2'(z_1)+s_2\psi_2'(z_2)\right]$$

where N_x^R, N_y^R and N_{xy}^R are remote applied stress resultants in x, y directions and xy plane, respectively. Considering $\rho=1$ for the edge of the cut out, we have;

$$\phi_2^{'}(z_1)=\frac{\phi_2^{'}(\zeta)}{\frac{dz_1}{d\zeta}}$$

$$\psi_2^{'}(z_2)=\frac{\psi_2^{'}(\zeta)}{\frac{dz_2}{d\zeta}}$$

$$\frac{dz_j}{d\zeta}=\frac{R}{2}\left[n_j\left(\frac{m}{\rho^2}-\frac{\rho^2}{\zeta^2}\right)+n_j^*\left(1-\frac{m}{\zeta^2}\right)\right]\xrightarrow{\rho=1}\frac{dz_j}{d\zeta}=\frac{R}{2}\left[n_j\left(m-\frac{1}{\zeta^2}\right)+n_j^*\left(1-\frac{m}{\zeta^2}\right)\right] \quad \text{(A19)}$$

$$\phi_2^{'}(\zeta)=-\frac{l_1}{\zeta^2}-\frac{l_2 m}{\zeta^2}$$

$$\psi_2^{'}(\zeta)=\frac{l_3}{\zeta^2}+\frac{l_4 m}{\zeta^2}$$

In order to transform stress resultants from Cartesian system to Curvilinear system, the following transformation is required [34];

$$\begin{aligned} &N_x+N_y=N_\theta+N_\rho \\ &N_\theta-N_\rho+2iN_{\rho\theta}=(N_y-N_x+2iN_{xy})e^{2i\alpha} \end{aligned} \quad \text{(A20)}$$

where N_θ, N_ρ and $N_{\rho\theta}$ are circumferential, radial and tangential stress resultants, respectively. The term $e^{2i\alpha}$ is defined as [34];

$$e^{2i\alpha}=\frac{\zeta^2}{\rho^2}\frac{\omega'(\zeta)}{\overline{\omega'(\zeta)}} \quad \text{(A21)}$$

Since no load is applied to the hole, only circumferential stresses can exist, i.e. $N_{\rho\theta}=N_\rho=0$, therefore;

$$N_x+N_y=N_\theta \quad \text{(A22)}$$

References

1. Makki MM, Chokri B. Experimental, analytical, and finite element study of stress concentration factors for composite materials. *J Compos Mater* 2017; 51: 1583–1594.

2. Kumar A, Agrawal A, Ghadai R, et al. Analysis of stress concentration in

orthotropic laminates. *Procedia Technol* 2016; 23: 156–162.

3. Jain NK, Mittal ND. Finite element analysis for stress concentration and deflection in isotropic, orthotropic and laminated composite plates with central circular hole under transverse static loading. *Mater Sci Eng A* 2008; 498: 115–124.

4. Henshaw JM, Sorem JR, Glaessgen EH. Finite element analysis of ply-by-ply and equivalent stress concentrations in composite plates with multiple holes under tensile and shear loading. *Compos Struct* 1996; 36: 45–58.

5. Haque A, Ahmed L, Ramasetty A. Stress concentrations and notch sensitivity in woven ceramic matrix composites containing a circular hole-an experimental, analytical, and finite element study. *J Am Ceram Soc* 2005; 88: 2195–2201.

6. Bonora N, Costanzi M, Marchetti M. A computational procedure to calculate stress-strain field around simple shape holes in composite laminates. *Comput Struct* 1994; 53: 1167–1179.

7. Bonora N, Costanzi M, Marchetti M. On closed form solution for the elastic stress field around holes in orthotropic composite plates under in-plane stress conditions. *Compos Struct* 1993; 25: 139–156.

8. Weißgraeber P, Felger J, Geipel D, et al. Cracks at elliptical holes: Stress intensity factor and Finite Fracture Mechanics solution. *Eur J Mech A/Solids* 2016; 55: 192–198.

9. Batista M. On the stress concentration around a hole in an infinite plate subject to a uniform load at infinity. *Int J Mech Sci* 2011; 53: 254–261.

10. Chauhan MM, Sharma DS, Dave JM. Stress intensity factor for hypocycloidal hole in finite plate. *Theor Appl Fract Mech* 2016; 82: 59–68.

11. Chauhan MM, Sharma DS. Stresses in finite anisotropic plate weakened by rectangular hole. *Int J Mech Sci* 2015; 101–102: 272–279.

12. Zappalorto M, Carraro PA. An engineering formula for the stress concentration factor of orthotropic composite plates. *Compos Part B Eng* 2015; 68: 51–58.

13. Russo A, Zuccarello B. An accurate method to predict the stress concentration in composite laminates with a circular hole under tensile loading. *Mech Compos Mater* 2007; 43: 359–376.

14. Hufenbach W, Grüber B, Gottwald R, et al. Analytical and experimental analysis of stress concentration in notched multilayered composites with finite outer boundaries. *Mech Compos Mater* 2010; 46: 531–538.

15. Muskhelishvili NI. *Some Basic Problems of the Mathematical Theory of Elasticity*. Springer Netherlands. Epub ahead of print 1977. DOI: 10.1007/978-94-017-3034-1.

16. Neuber H. G. N. Savin, Stress Concentration around Holes. XI + 430 S. m. 208 Abb. u. 77 Tafeln. Oxford/London/New York/Paris 1961. Pergamon Press. Preis geb. 84 s. net. *ZAMM - Zeitschrift für Angew Math und Mech* 1962; 42: 265–265.

17. Sharma DS. Stresses around polygonal hole in an infinite laminated composite plate. *Eur J Mech A/Solids* 2015; 54: 44–52.

18. Ukadgaonker VG, Rao DKN. Stress distribution around triangular holes in anisotropic plates. *Compos Struct* 1999; 45: 171–183.

19. Jafari M, Ardalani E. Stress concentration in finite metallic plates with regular holes. *Int J Mech Sci* 2016; 106: 220–230.

20. Sharma DS. Moment distribution around polygonal holes in infinite plate. *Int J Mech Sci* 2014; 78: 177–182.

21. Ukadgaonker VG, Rao DKN. A general solution for stresses around holes in symmetric laminates under inplane loading. *Compos Struct* 2000; 49: 339–354.

22. Ukadgaonker VG, Kakhandki V. Stress analysis for an orthotropic plate with an

irregular shaped hole for different in-plane loading conditions - Part 1. *Compos Struct* 2005; 70: 255–274.

23. Jain NK, Mittal ND. Finite element analysis for stress concentration and deflection in isotropic, orthotropic and laminated composite plates with central circular hole under transverse static loading. *Mater Sci Eng A* 2008; 498: 115–124.

24. Khechai A, Tati A, Guettala A. Finite element analysis of stress concentrations and failure criteria in composite plates with circular holes. *Front Mech Eng* 2014; 9: 281–294.

25. Othman A, Jadee KJ, Ismadi M-Z. Mitigating stress concentration through defense hole system for improvement in bearing strength of composite bolted joint, Part 1: Numerical analysis. *J Compos Mater* 2017; 51: 3685–3699.

26. Darwish F, Gharaibeh M, Tashtoush G. A modified equation for the stress concentration factor in countersunk holes. *Eur J Mech A/Solids* 2012; 36: 94–103.

27. Darwish F, Tashtoush G, Gharaibeh M. Stress concentration analysis for countersunk rivet holes in orthotropic plates. *Eur J Mech A/Solids* 2013; 37: 69–78.

28. Zhao GH, Tong JW, Shen M. Numerical Analysis and Experimental Validation of Interlaminar Stresses of Quasi-isotropic APC-2/AS-4 Laminate with a Central Hole Loaded in Tension. *J Thermoplast Compos Mater* 2010; 23: 413–433.

29. Microsoft. Excel.

30. MSC Software Corporation. Nastran 2016.

31. Kassapoglou C. *Review of laminate strength and failure criteria*. 2nd ed. Hoboken, N.J. : Wiley ; Chichester : John Wiley [distributor], 2013. Epub ahead of print 2013. DOI: 10.1002/9781118536933.

32. Pandita SD, Nishiyabu K, Verpoest I. Strain concentrations in woven fabric composites with holes. *Compos Struct* 2003; 59: 361–368.

33. Lekhnitskii SG. *Theory of elasticity of an anisotropic elastic body*. San Francisco-Holden-Day Inc, 1963.

34. Pan Z, Cheng Y, Liu J. Stress analysis of a finite plate with a rectangular hole subjected to uniaxial tension using modified stress functions. *Int J Mech Sci* 2013; 75: 265–277.

Table 1: CFRP material used for results generation

Material	E_{11} (GPa)	E_{22} (GPa)	G_{12} (GPa)	υ_{12}	t (mm)
Hexcel 8552 AS4 unidirectional prepreg at 190gsm	120.00	10.00	5.58	0.305	0.18

Table 2: Material and lay-up used for FEA validation

Validation ID	Material	Lay-up/ Loading	Hole shape	E_{11} (GPa)	E_{22} (GPa)	G_{12} (GPa)	υ_{12}
Val-A	Hexcel 8552S AS4 3K Plain Weave Fabric	$(45/0/-45/90/0)_s$ / bi-axial	Circular (a=10 mm, b=10 mm)	62.00	62.00	4.20	0.05
Val-B		$(45/0/-45/90/0)_s$ / uni-axial	Elliptical (a=20 mm, b=10 mm)				

Table 3: Mechanical properties of purely angle ply laminates

Stacking sequence	E_x (GPa)	E_y (GPa)	E_x / E_y	G_{xy} (GPa)	υ_{xy}	υ_{yx}
$((15/-15)_7)_s$	99.04	10.26	9.66	12.00	0.09	0.85
$((30/-30)_7)_s$	47.24	11.84	3.99	24.82	0.30	1.20
$((45/-45)_7)_s$	19.20	19.20	1.00	31.23	0.72	0.72
$((60/-60)_7)_s$	11.84	47.24	0.25	24.82	1.20	0.30
$((75/-75)_7)_s$	10.26	99.04	0.10	12.00	0.85	0.09

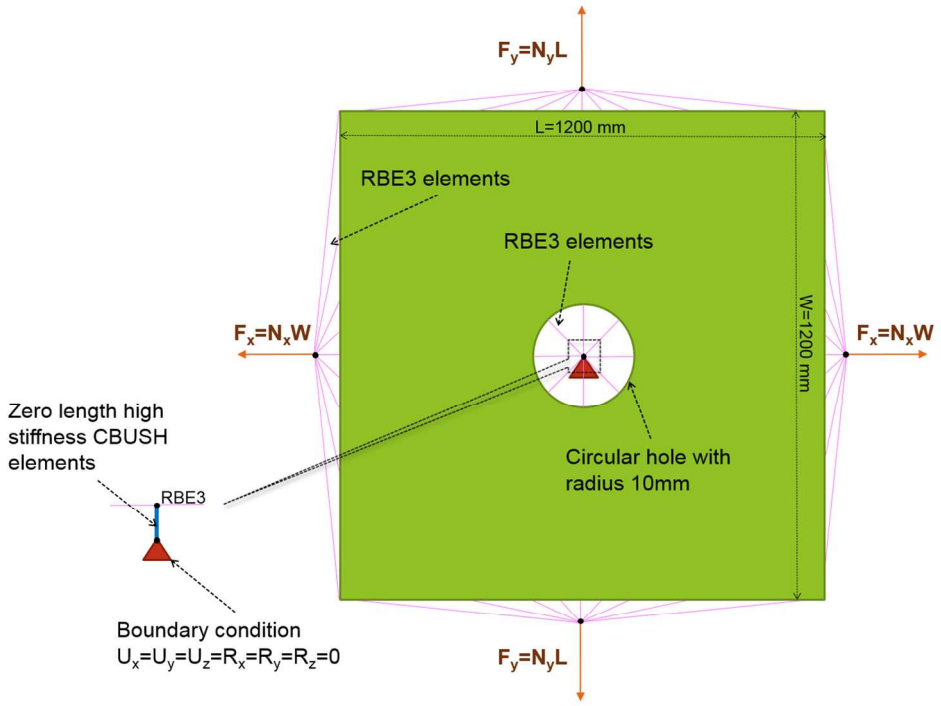

Fig. 1: Schematic representation of geometry, loading and boundary condition for FEA

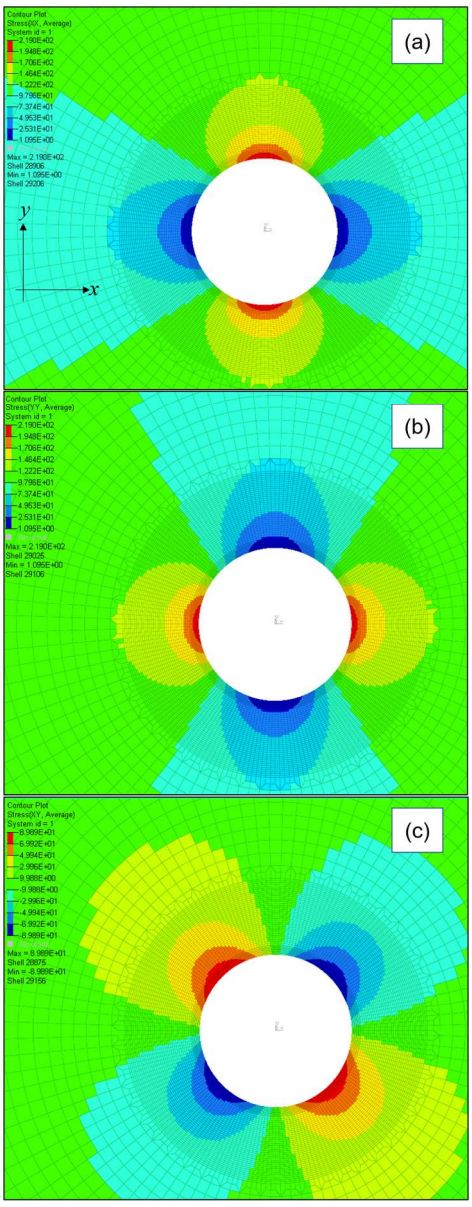

Fig. 2: Contour plot of stresses for an infinite composite plate containing a circular hole of radius 10mm under bi-axial loading (Val-A), i.e. N_x=N_y=280N/mm; (a) Normal stress in x-direction, (b) Normal stress in y-direction and (c) Shear stress in xy plane

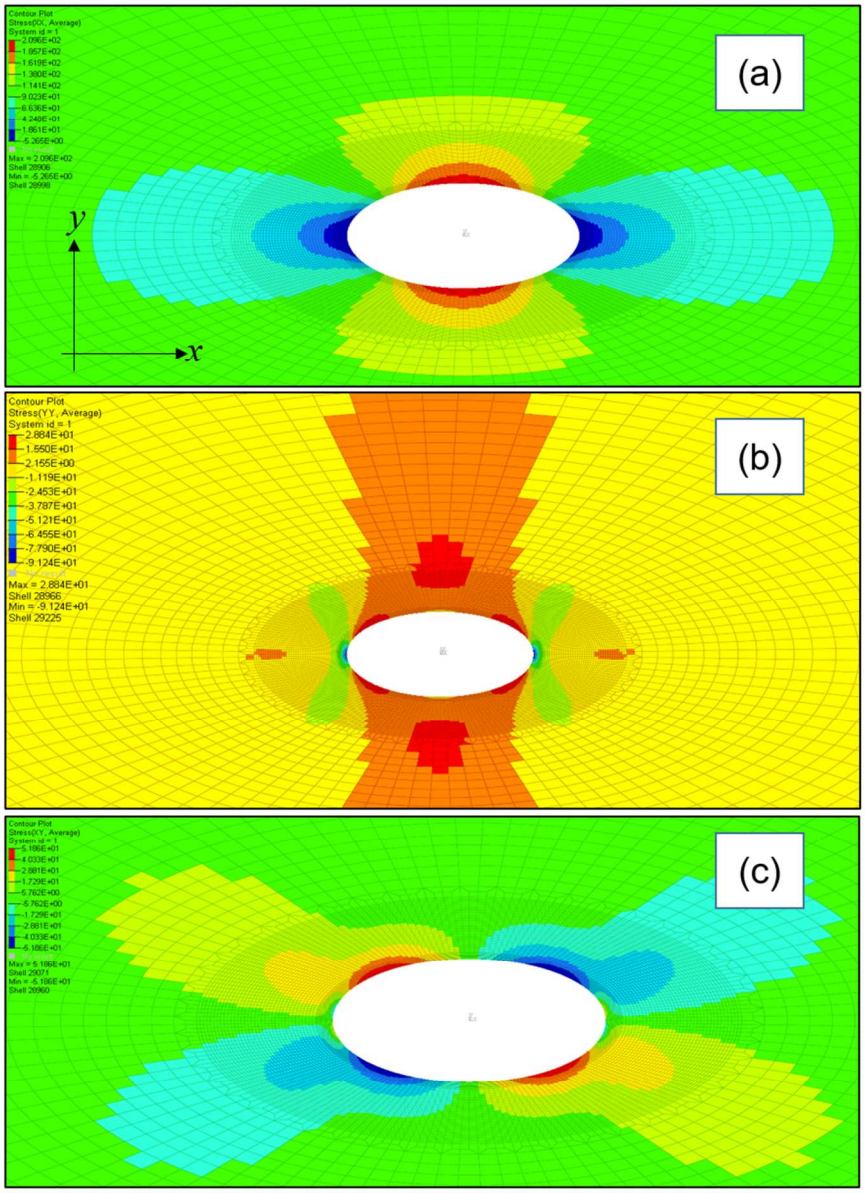

Fig. 3: Contour plot of stresses for an infinite composite plate containing an elliptical hole of radius 10mm under uni-axial loading (Val-B), i.e. N_x=280N/mm; (a) Normal stress in x-direction, (b) Normal stress in y-direction and (c) Shear stress in xy plane

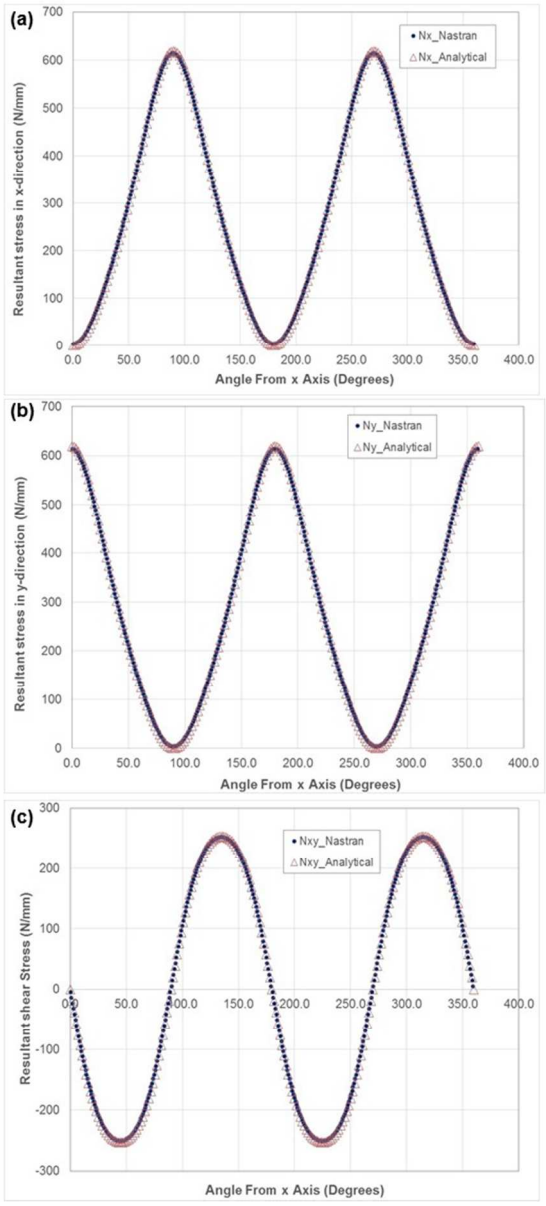

Fig. 4: Comparison of stress resultant output at the edge of a circular hole for both analytical and FE approaches, i.e. Normal stress resultant in (a) *x*-direction and (b) *y*-direction and (c) shear in *xy* plane

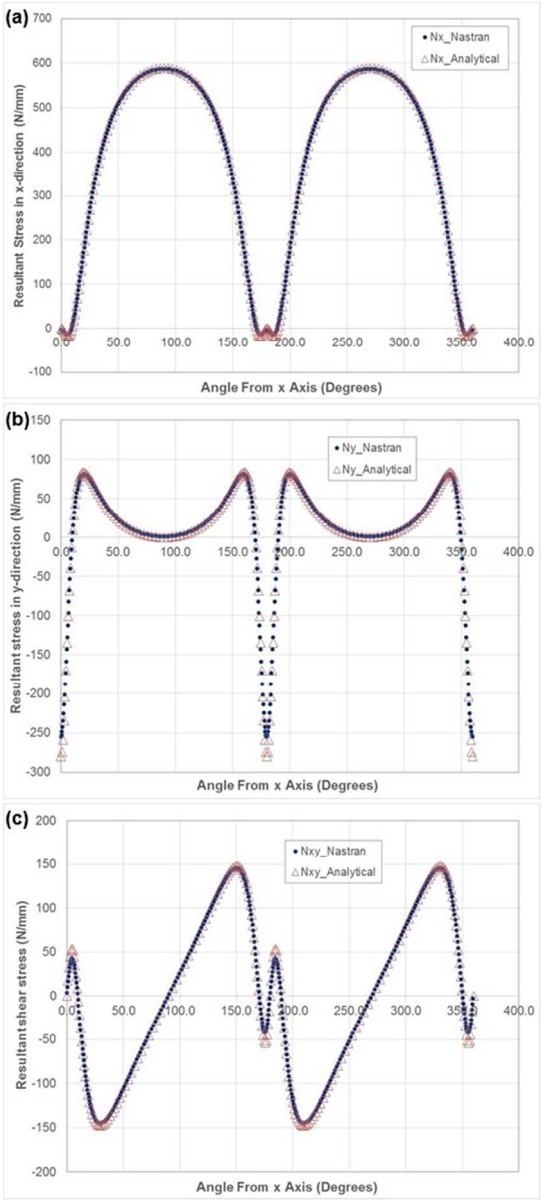

Fig. 5: Comparison of stress resultant output at the edge of an elliptical hole for both analytical and FE approaches, i.e. Normal stress resultant in (a) *x*-direction and (b) *y*-direction and (c) shear in xy plane

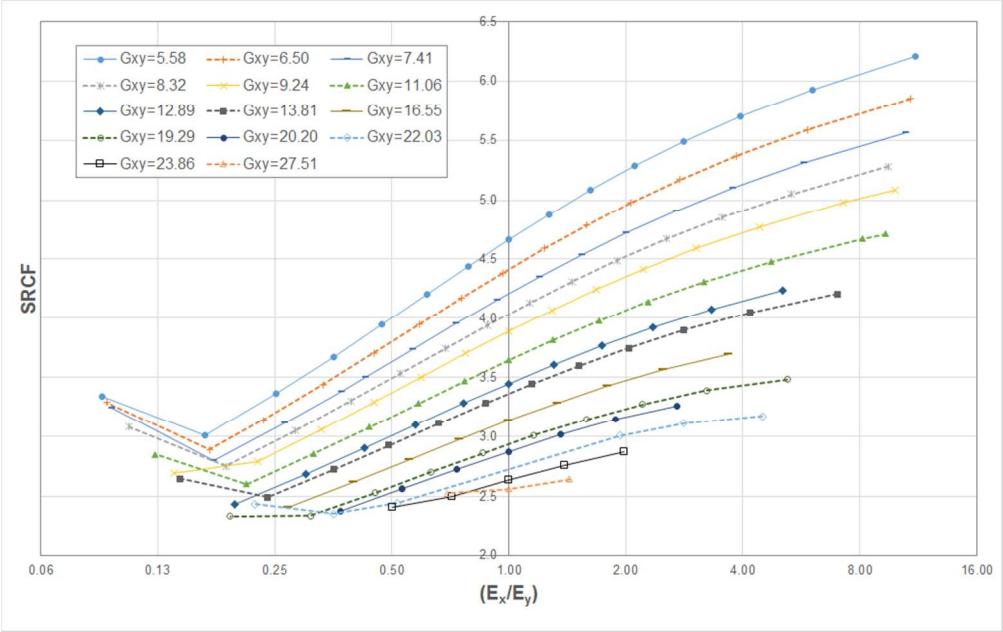

Fig. 6: Semi-log plot of SRCF vs E_x/E_y for loading λ=0. Unit of stiffness is GPa

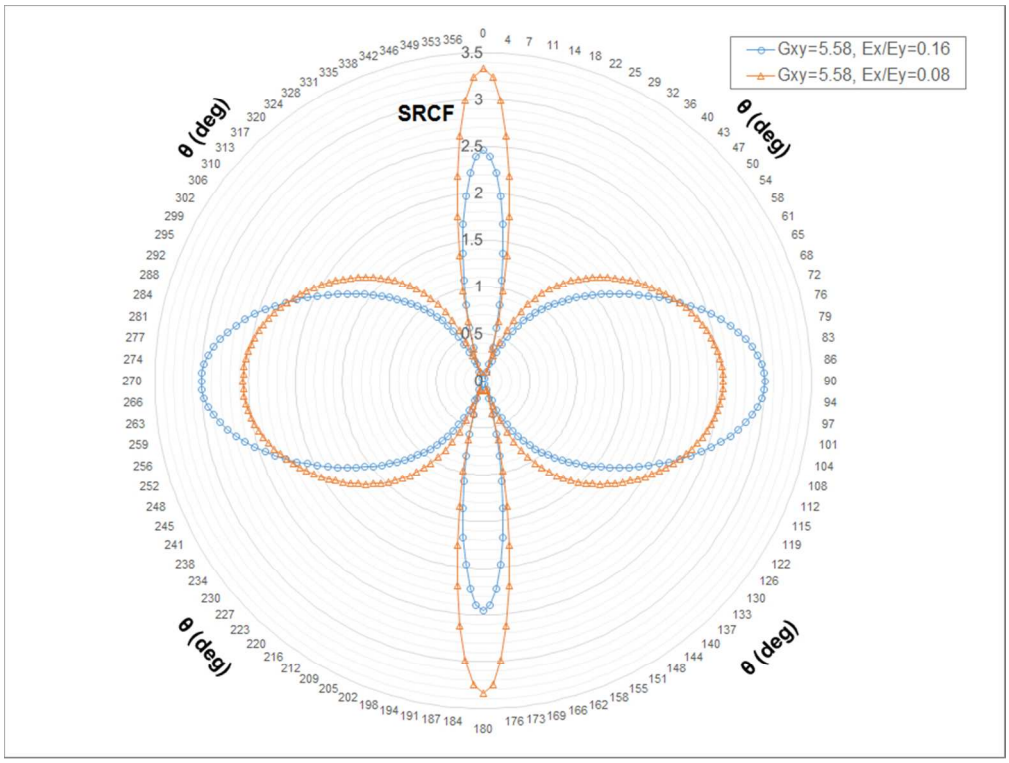

Fig. 7: Distribution of the SRCF around the edge of the hole for uni-axial loading for G_{xy}=5.58GPa for stacking sequences of $(90_{13}/0)_s$ and $(90)_{28}$ associated to E_x/E_y of 0.16 and 0.08, respectively. The load is applied at 0^o direction

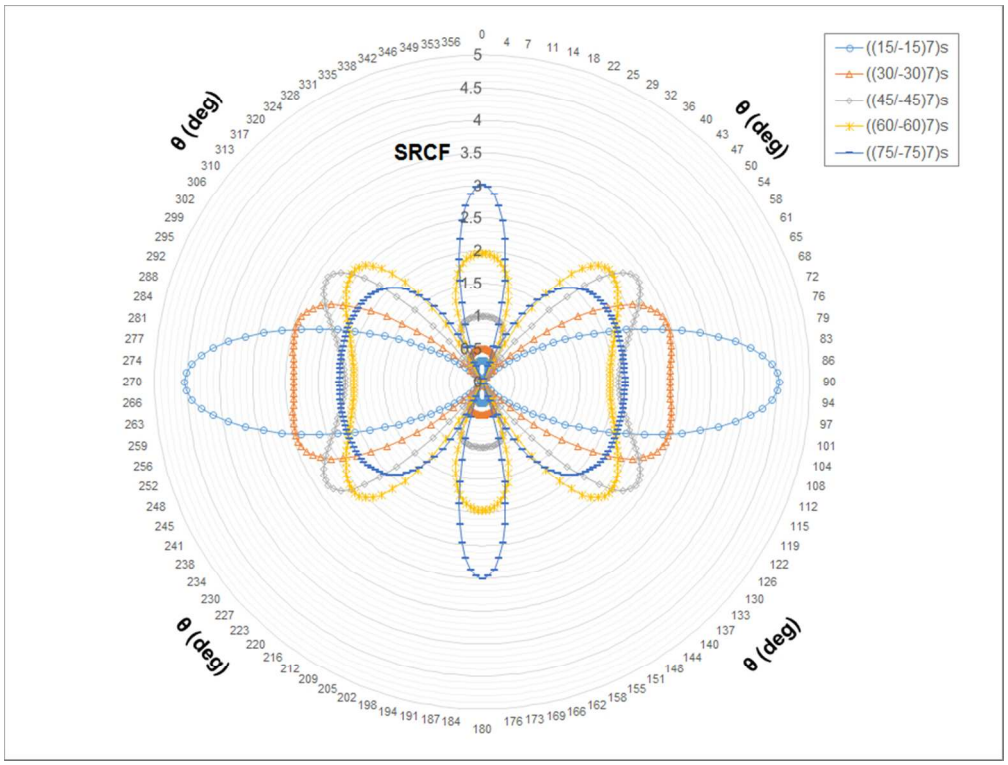

Fig. 8: Plot of SRCF E_x/E_y for loading λ=0 and angle ply sequences only

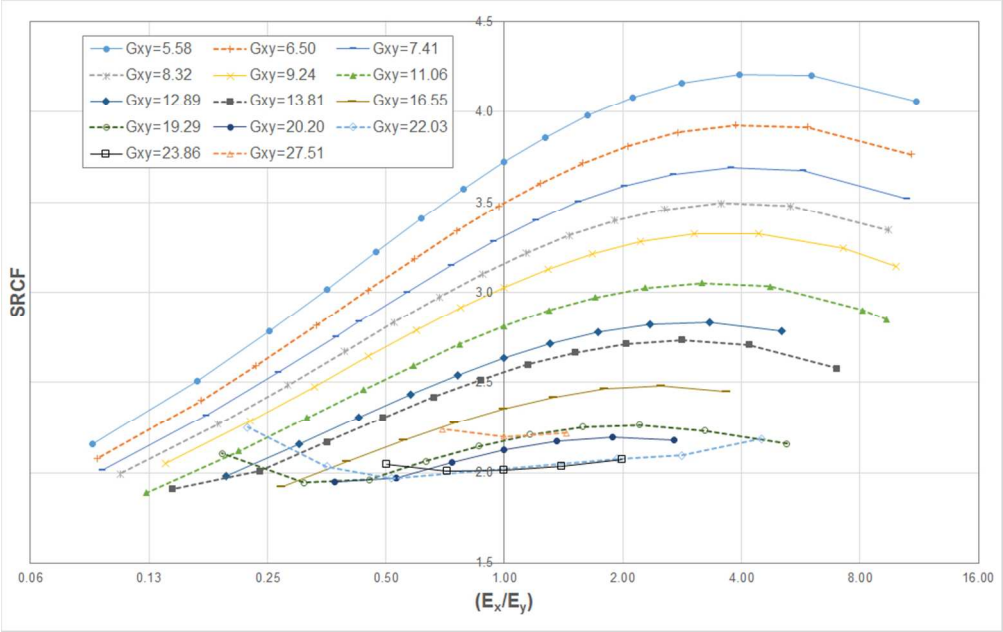

Fig. 9: Semi-log plot of SRCF vs E_x/E_y for loading λ=0.5. Unit of stiffness is GPa

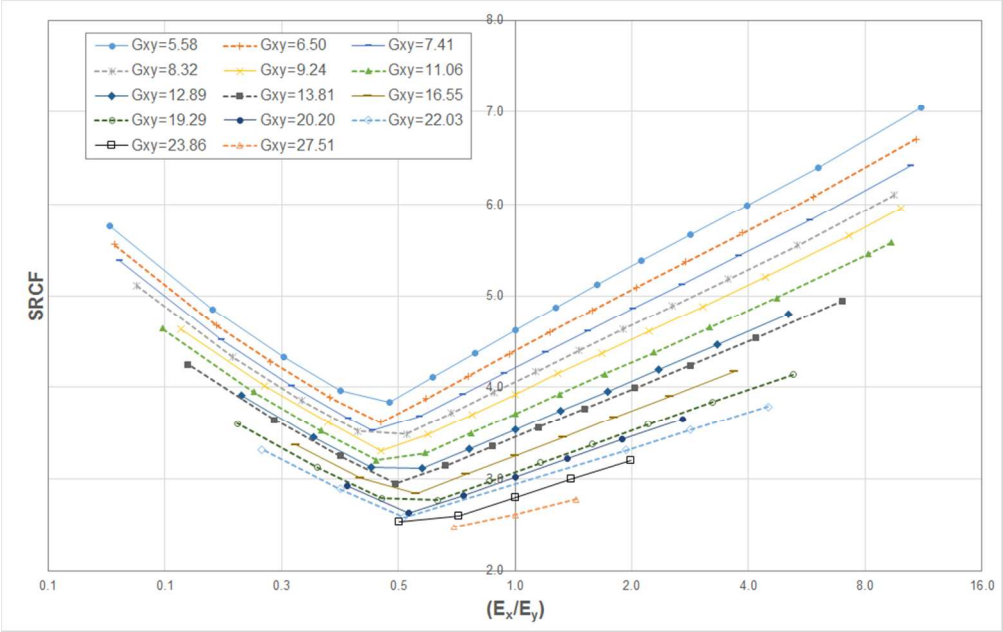

Fig. 10: Semi-log plot of SRCF vs E_x/E_y for loading λ=-0.5, N_x is in tension and N_y is in compression. Unit of stiffness is GPa

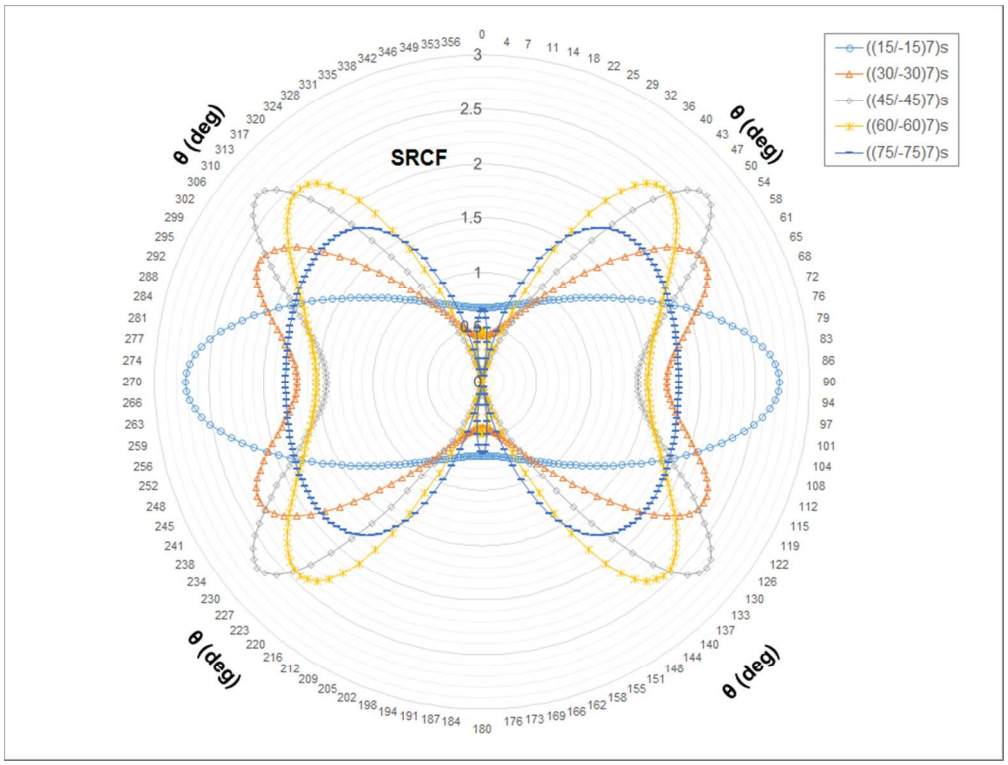

Fig. 11: Plot of SRCF vs E_x/E_y for loading λ=0.5 for angle ply sequences only

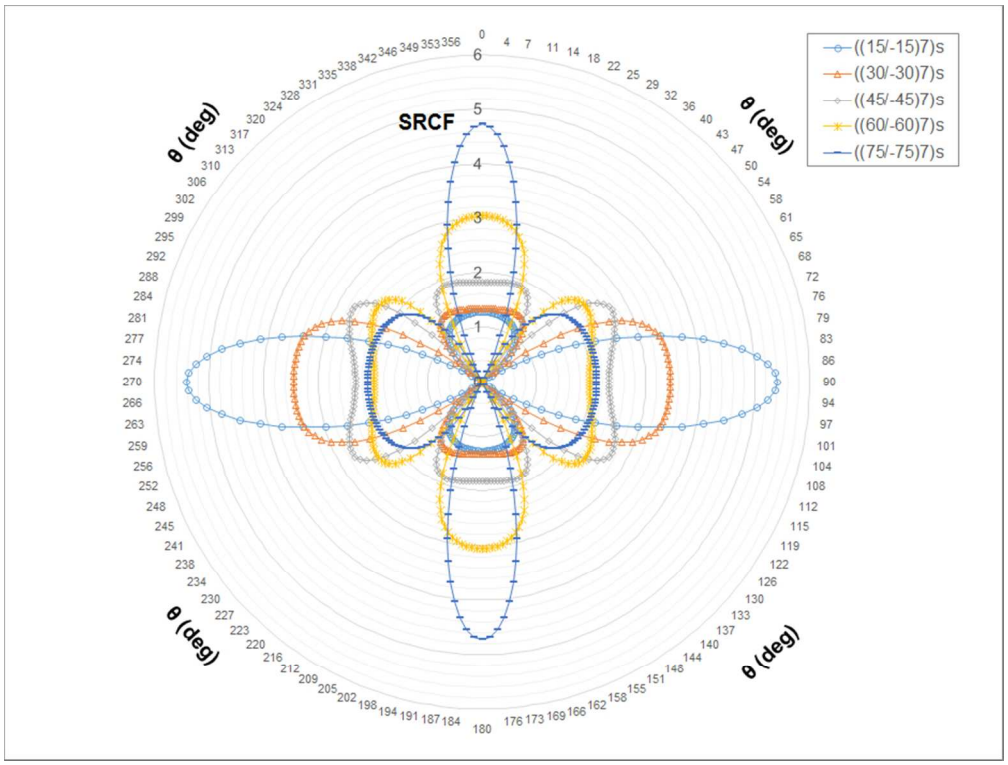

Fig. 12: Plot of SRCF vs E_x/E_y for loading λ=-0.5 for angle ply sequences only

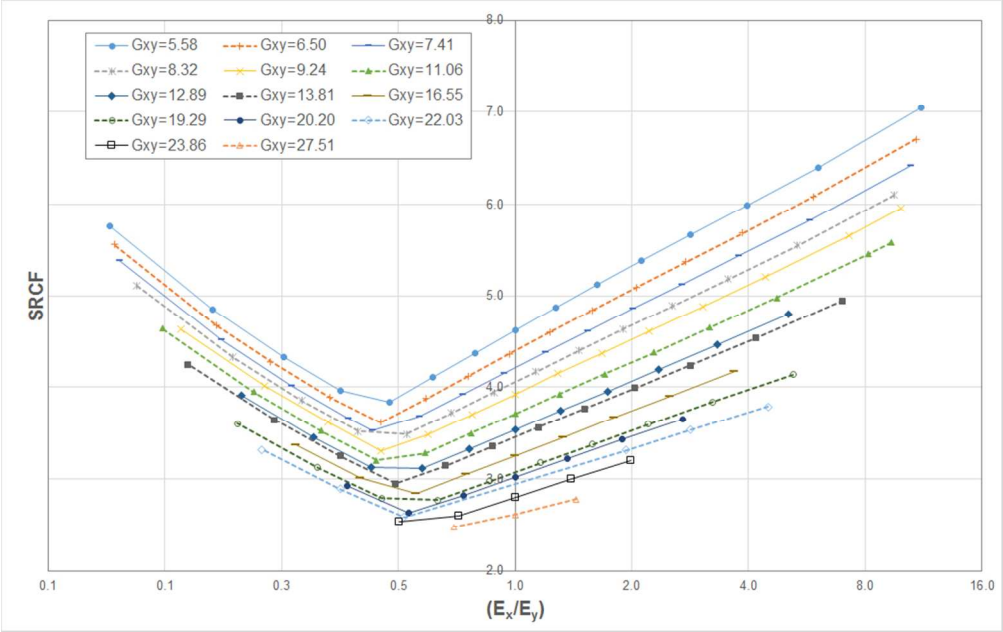

Fig. 13: Semi-log plot of SRCF vs E_x/E_y for loading λ=-1.00. Unit of stiffness is GPa

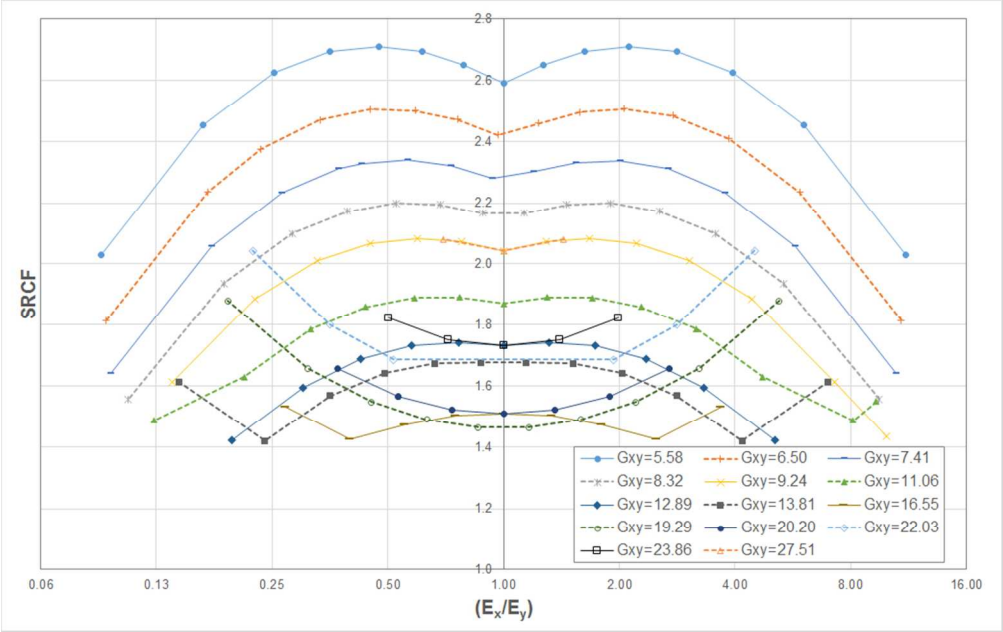

Fig. 14: Semi-log plot of SRCF vs E_x/E_y for loading λ=1.00. Unit of stiffness is GPa

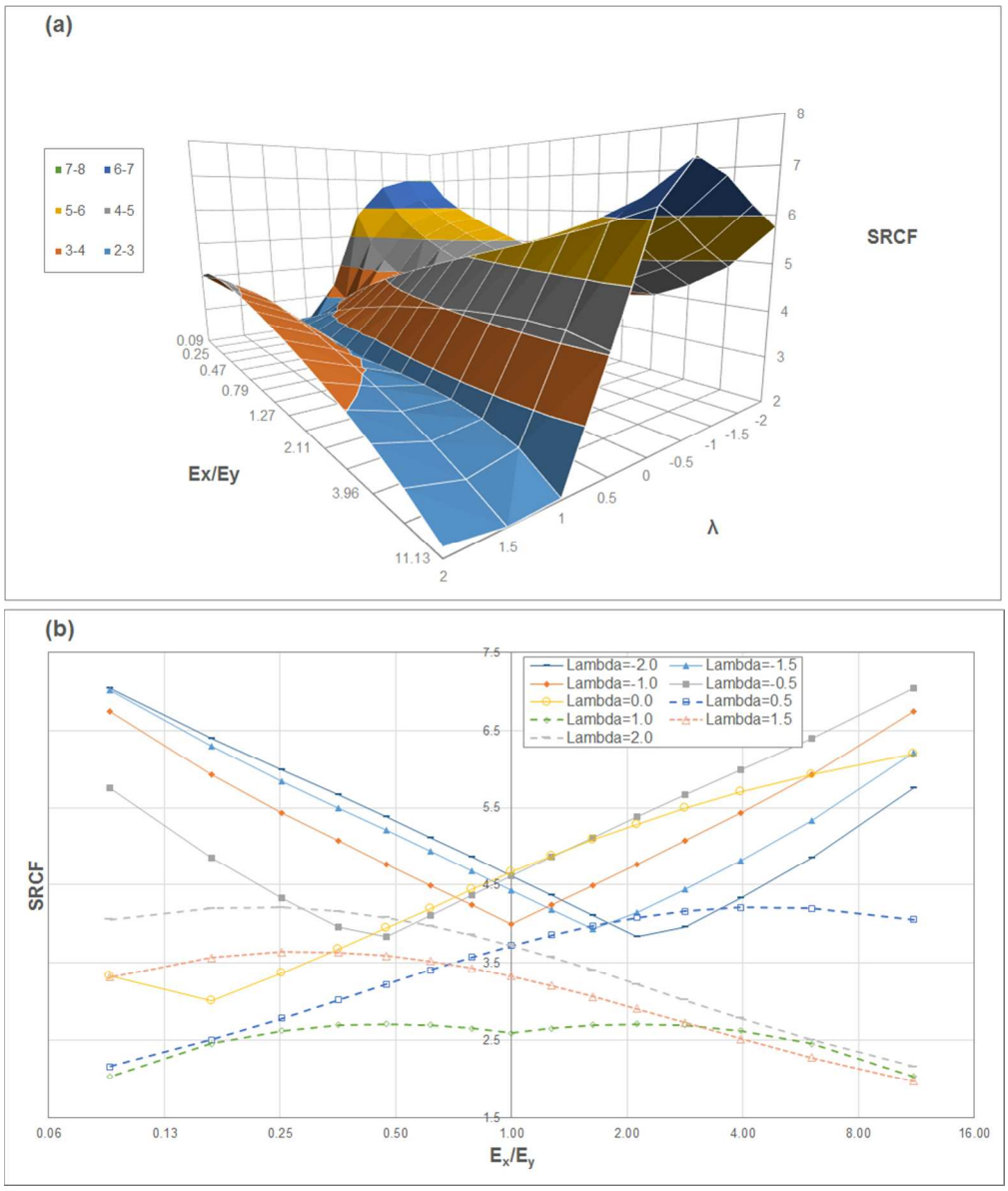

Fig. 15: Graphs of SRCF for various E_x/E_y and load ratio λ for laminates with G_{xy}=5.58GPa, (a) 3D surface graph and (b) semi-logarithmic 2D graph

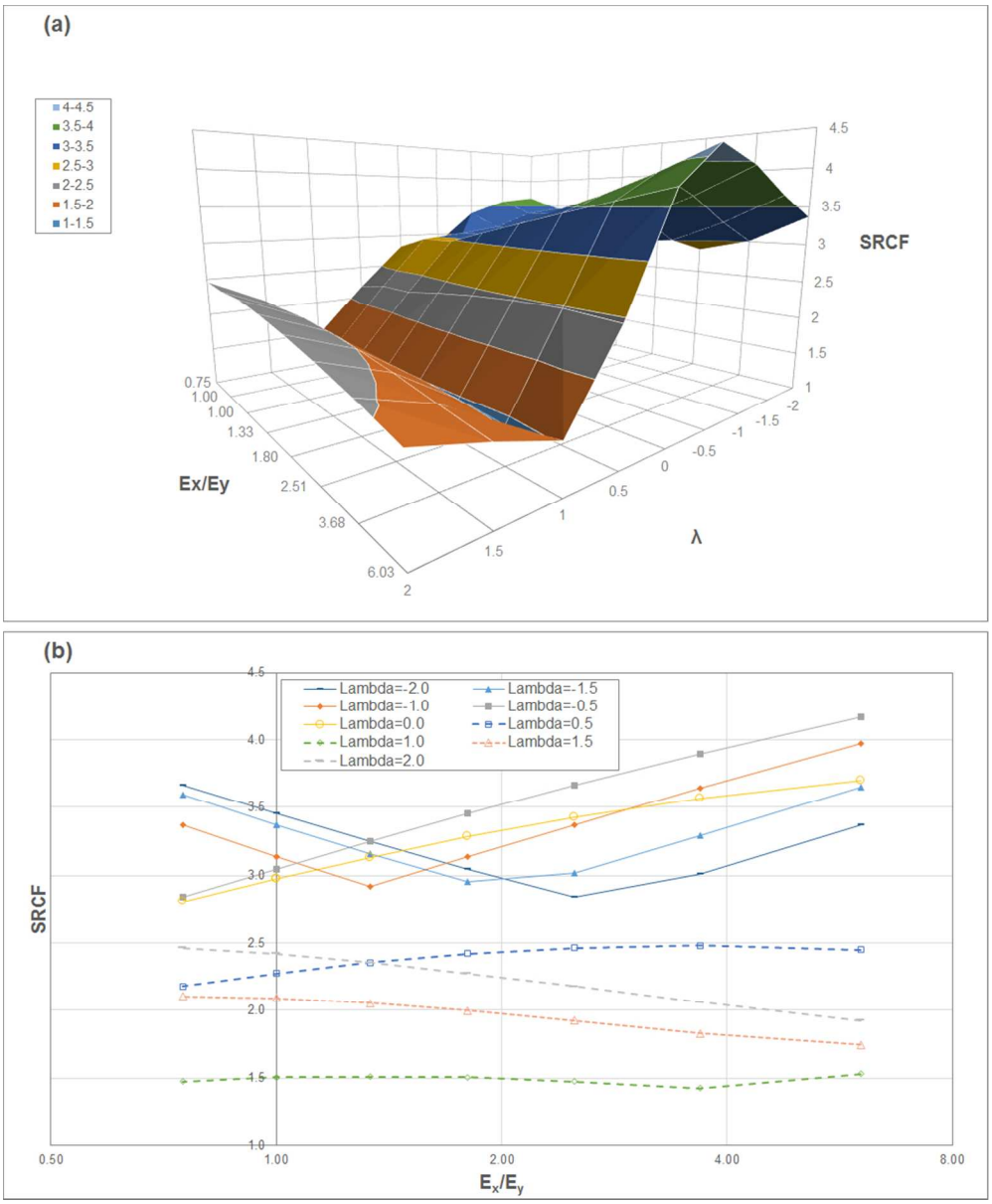

Fig. 16: Graphs of SRCF for various E_x/E_y and load ratio λ for laminates with G_{xy}=16.58GPa, (a) 3D surface graph and (b) semi-logarithmic 2D graph

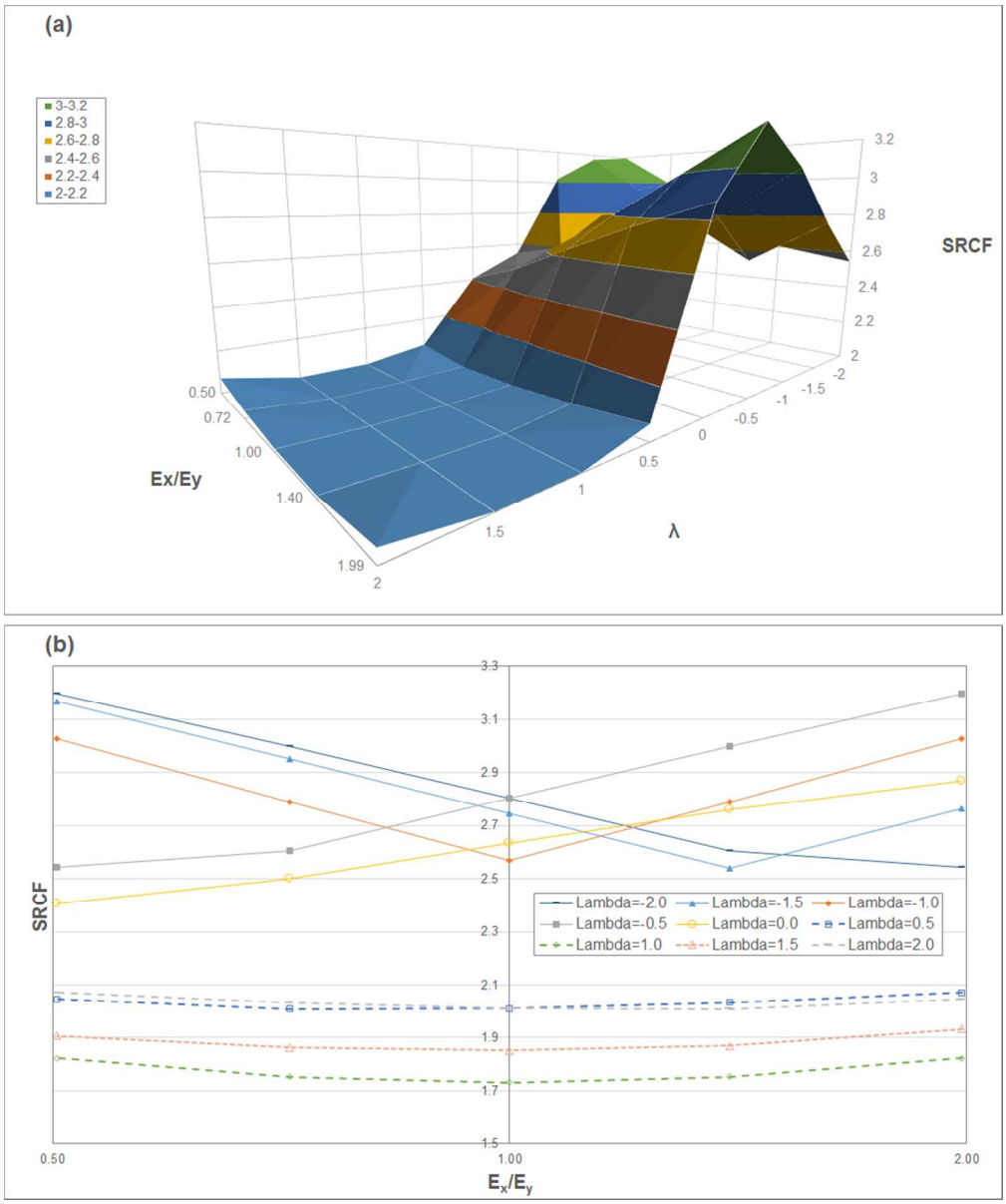

Fig. 17: Graphs of SRCF for various E_x/E_y and load ratio λ for laminates with G_{xy}=23.86GPa, (a) 3D surface graph and (b) semi-logarithmic 2D graph

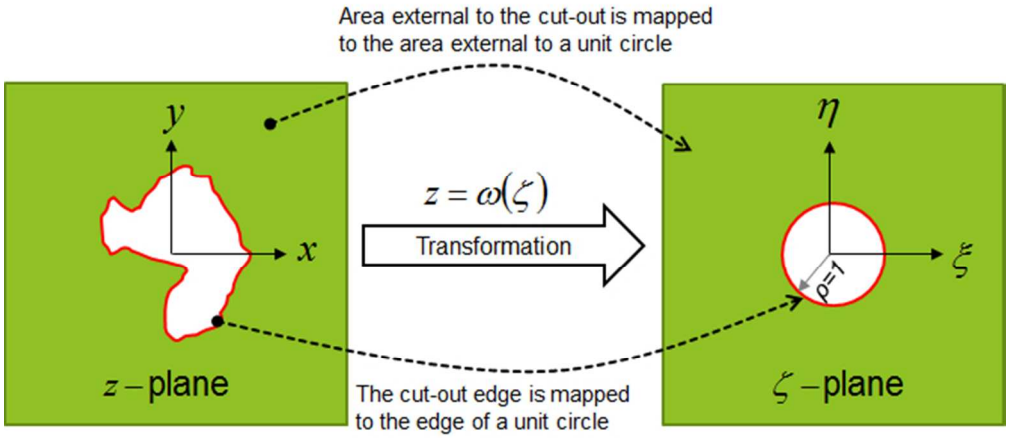

Fig. A1: Illustration of mapping a hole having an irregular shape in an infinite plate onto a unit circle using mapping functions

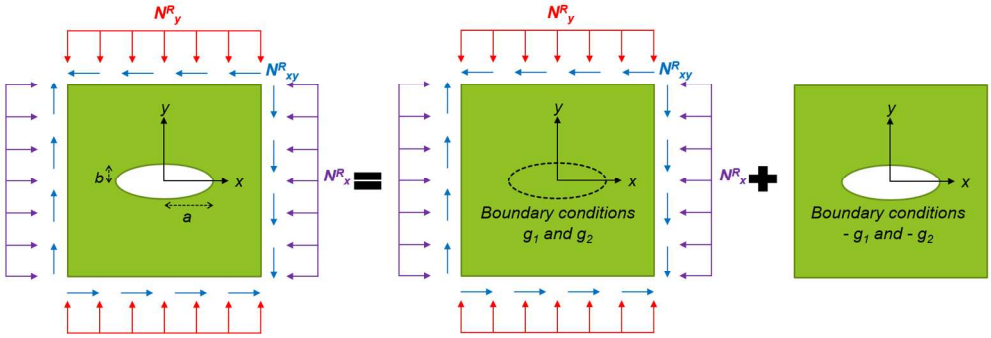

Fig. A2: Use of principle of superposition for calculation of stress functions